

# **Drive-induced Non-local Interactions and Topological Bulk Transport of Extended Doublons**

**Julius Beck<sup>1</sup>, Matthias Heinrich<sup>1</sup>, Marcus J. Meschede<sup>1</sup>, Helena Drüeke<sup>1</sup>,**

**Francesco S. Piccioli<sup>1,2</sup>, Sebastian Weidemann<sup>1</sup>, Joshua Feis<sup>1</sup>**

**Dieter Bauer<sup>1</sup>, and Alexander Szameit<sup>1</sup>**

*<sup>1</sup> Institute of Physics, University of Rostock, Albert-Einstein-Str. 23, 18059 Rostock, Germany.*

*<sup>2</sup> INO-CNR BEC Center and Dipartimento di Fisica, Università di Trento, Via Sommarive 14, 38123 Povo, Italy.*

The existence of boundary states and their protection against symmetry-preserving perturbations are a hallmark feature of topological systems. While this concept originally emerged in the context of single-particle phenomena in condensed-matter physics, particle interactions have recently been identified as alternative means to establish topological phases. As a consequence, nonlinear topological insulators gained much interest as a model system for many interacting particles. However, as their mean-field model inevitably breaks down for small numbers of particles, to date, topological states composed of only few interacting particles remain experimentally largely unexplored. In our work, we explore the physics of extended interaction-induced two-particle topological states, so-called Doublons. We experimentally implement non-local- interactions via non-adiabatic periodic driving and dimensional mapping in an artificial photonic solid. The resonant formation of extended Doublon quasi-particles at specific local interaction strengths is observed, allowing us to probe the topologically protected motion of these entities through the bulk of the system. Our approach is compatible to a number of established experimental platforms and paves the way for studying topological few-particle phenomena with finite interaction strength.

Shortly after their discovery<sup>1,2</sup> and subsequent first experimental demonstration<sup>3</sup>, topological insulators began to attract substantial interest by virtue of their peculiar properties, in particular their signature feature of scattering-immune protected edge currents<sup>4</sup>. Today, topological insulators, and topological transport in general, are no longer exclusive to condensed-matter systems<sup>5</sup>, but have become a staple in numerous other wave-physical systems, such as cold atoms<sup>6,7</sup>, electric circuits<sup>8,9</sup>, mechanical waves<sup>10</sup>, acoustics<sup>11</sup>, and photonics<sup>12,13</sup>. This wide variety of available platforms provides exceptional conditions for different methods of establishing non-trivial topology to be explored and honed, such as anomalous driving<sup>14–16</sup>, non-Hermitian topology<sup>17,18</sup>, quantum topology<sup>19,20</sup>, adiabatic Thouless pumping<sup>21–23</sup>, and nonlinear topological systems<sup>9,24–26</sup>. In particular, nonlinear systems play a pivotal role in the understanding of many-body topological phenomena as interaction forces between many particles can be mapped onto nonlinear terms using mean-field approaches. The prototypical example is the Gross-Pitaevskii equation<sup>27</sup>, where a nonlinear Kerr term is added to a single-particle Schrödinger equation in order to describe the average dynamics resulting from collisions<sup>9,25,28</sup>.

On the opposite end of the spectrum, the existence of topological dynamics of interacting few-particle systems have been studied, with a particular focus on bipartite quasi-particles, dubbed “Doublons”<sup>29</sup>. These entities are defined as metastable states of two interacting particles with either repulsive<sup>29</sup> or attractive forces<sup>30,31</sup>. Doublons show a number of peculiar features: They exhibit an extraordinary long lifetime even when experiencing intra-state collisions<sup>29</sup>. The existence of Doublons also facilitates many-body localization in disordered<sup>30</sup> and generalized<sup>32</sup> Hubbard models. Topologically protected Doublon boundary states may exist at parameter regimes where single particle systems are topologically trivial<sup>33,34</sup>. Moreover, very large interactions may break the famous bulk-boundary correspondence<sup>33,34</sup>, such that it had to be extended to an interacting two-particle formalism<sup>35</sup>. Last but not least, topological Doublons can be interpreted as generalized W states for a system of qutrits which enables the investigation of many body quantum correlations<sup>36</sup>. In previous experimental implementations, Doublons were simplified as doubly occupied lattice sites<sup>29–31,37–41</sup>. However, this captures only a small fraction of the Doublon physics as these entities are defined as bound bipartite quasi-particles with long-range interaction<sup>42,43</sup>. As a consequence, in its most general form, a Doublon can potentially extend over several lattice sites. To date, the rich physics of this fundamental property remains experimentally unexplored.

In our work, we experimentally explore the physics of extended Doublon quasi-particles. We induce their non-local interaction by combining a non-adiabatic drive with dimensional mapping. Using a photonic artificial solid, we show the formation of Doublons at certain resonances in the interaction strength and their topologically protected motion through the bulk of the system.

Our approach is summarized in Fig. 1. We start with a Su-Schrieffer-Heeger chain<sup>44,45</sup> characterized by alternating weak and strong bonds between the individual lattice sites, and place two distinguishable particles that exhibit a local (i.e., hard-shell) interaction. This system is governed by the Hamiltonian

$$\hat{H} = \hat{H}_0 + \hat{H}_{\text{int}},$$

where  $\hat{H}_0$  describes the individual dynamics of each particle under nearest-neighbor hopping, and  $\hat{H}_{\text{int}}$  accounts for their local interaction. As explained in detail in the Supplementary Information,  $\hat{H}_0$  can be expanded into four virtual Hamiltonians  $\hat{H}_I, \dots, \hat{H}_{IV}$ ,

$$\hat{H}_0 = \hat{H}_I + \hat{H}_{II} + \hat{H}_{III} + \hat{H}_{IV} ,$$

that, individually, consist exclusively of non-local interaction terms, while in the summation, these interactions cancel in accordance with the properties of Hamiltonian  $\hat{H}_0$ . Crucially, this mutual cancellation in the summation only occurs if the four virtual Hamiltonians act simultaneously. The situation changes dramatically if the system is driven in a way that sequentially enables these constituent Hamiltonians at different time steps. Evading cancellation in this manner allows for the non-local interaction terms to physically manifest themselves and to imprint their signatures onto the particles' dynamics where they can be directly observed. To this end, our non-adiabatic drive establishes different delays on the individual virtual Hamiltonians. As we will show in the following, drive-induced non-local interactions indeed facilitate the formation of extended Doublons. Moreover, our protocol suggests that the bulk dynamics of these quasiparticles is of topological origin and, hence, robust to perturbations. As was shown before<sup>37,46</sup>, two particles with local interaction moving on a one-dimensional (1D) lattice can be mapped onto the evolution of a single particle in a two-dimensional (2D) square lattice system by interpreting the position coordinates of the two particles in the 1D lattice as the two Cartesian coordinates of a single particle in a square 2D lattice. In turn, the local Hubbard interaction strength in the 1D system is mapped onto a detuning of the diagonal sites of the 2D system (Fig. 2a).

The prerequisite non-adiabatic drive is imposed by means of the protocol depicted in Fig. 2b. While the on-site potential remains constant over the entire Floquet period  $T$ , coupling to each of a lattice site's four neighbors is selectively enabled in one of the four discrete steps for  $T/4$  in clockwise order. Interestingly, as we detail in the Supplementary Information section, the rationale of the mapping procedure from 1D to 2D not only remains unaffected in the presence of such a drive, but each step of the protocol actually instantiates one of the previously virtual Hamiltonians  $\hat{H}_I, \dots, \hat{H}_{IV}$ . Whereas in the static system, the non-local characteristics are veiled by the cancellation of these coexisting Hamiltonians, the helical drive serves to reveal the essence of the resulting extended quasi-particle dynamics. In each step, the position of one of the particles determines which inter-site hoppings of the analogous 1D lattice promote the dynamics of the other.

A perhaps more widely known consequence of the helical drive is its analogue to time-reversal symmetry-breaking that renders the lattice topologically non-trivial as indicated by non-vanishing winding numbers<sup>47</sup>. Along these lines, recent implementations of anomalous topological insulators<sup>14–16</sup>,  $\mathbb{Z}_2$  topological insulators<sup>48</sup>, and even PT-symmetric topological insulators<sup>17</sup> have been reported. In the context of our mapping procedure, we note that anomalous topological edge states persist in the presence of local perturbations such as detuned diagonal sites of

the square lattice. Moreover, since the topological characteristics of a lattice are unaffected by its shape, a triangular lattice domain subjected to the same drive equally supports topological edge states along its perimeter. This situation corresponds to an infinitely detuned diagonal that essentially bisects the square lattice into two uncoupled triangular domains as any hopping between the two lattices is fully suppressed. In other words, topological edge states can also travel within channels directly adjacent to the detuned diagonal. Viewed through the lens of the mapping procedure, they correspond to a state where the two particles are bound together, as both their coordinates jointly increase or decrease, respectively (see Fig. 3d). Yet, despite clearly being of topological origin, the two-particle state happens to traverse the bulk of the analogous 1D system. Even the sign of the interaction does not play a role: Both positive and negative detunings (corresponding to repulsive and attractive forces) result in the formation of such a state.

As it turns out, these topological bulk states may also exist for finite interaction strengths between the two particles<sup>36,49</sup>. Figure 3a shows the hopping probability  $p(U)$  onto the lattice diagonal as a function of the detuning  $U$  of the diagonal sites. While its envelope decays toward zero for infinitely strong detunings,  $p(U)$  exhibits an oscillatory behavior and vanishes for specific values of  $U$ . As a consequence, the two triangular lattices are once more effectively decoupled and support the aforementioned topological channels. This interpretation is supported by the band structure of our system depicted in Figs. 3b-d. In the trivial case without detuning on the diagonal ( $p(0) = 1$ ) an anomalous edge state bifurcates from the degenerate flat bands at zero energy. At the first zero of the hopping probability ( $p(2\sqrt{3}) = 0$ ) the lattices above and below the detuned diagonal are decoupled, resulting in additional interface channels with corresponding edge bands. In turn, the states on the diagonal sites remain localized in the detuned flat band. For off-resonant detunings ( $p(U) > 0$ ), a superposition of three interface bands displaying avoided crossings are present until the interface bands and the conventional edge bands eventually overlap in energy at  $U \rightarrow \infty$ .

For our experiments, we implemented our driven lattices on a photonic platform: Evanescently coupled integrated photonic waveguides fabricated via the femtosecond laser direct-write technique<sup>50</sup> (see Methods). The evolution of light in waveguide lattices is governed by a set of tight-binding equations that are analogous to the discrete Schrödinger equations known from condensed matter physics. The main distinction, however, is that the time coordinate  $t$  is replaced by the spatial propagation coordinate  $z$  along the waveguides in the photonic system. The non-adiabatic drive, hence, can be established through a modulation of the inter-site hopping along the waveguide structure in a chiral fashion that breaks the  $z$ -reversal symmetry of the system.

In Fig. 4, we present a summary of our measurements of the Doublon dynamics with finite interaction strength at the first resonance. The technical details of the measurements are listed in the Methods section. The system was probed incrementally by single-site excitations along the off-diagonal of the square lattice of waveguides at different positions in each panel. After two full Floquet periods, the wave packet has propagated over four sites, that is, two unit cells, in clockwise direction along the edge in line with the four virtual Hamiltonians  $\hat{H}_I, \dots, \hat{H}_{IV}$ : In

each step, one of the two particles remains at rest and, in doing so, determines the dynamics of the second particle, irrespective of their distance. Illustrating the key signature of a Doublon, this motion, however, is quite non-trivial due to the strictly non-local interaction: In our particular implementation, one particle moves by one lattice site only when the second particle is resting in the neighboring site, whereas the second particle moves only when the first particle is resting two lattice sites away. Crucially, this motion is inherently topological, as the excitation populates an anomalous topological edge state that travels along the detuned diagonal in the mapped 2D system.

A detailed comparison of the Doublon dynamics at different interaction strengths, that is, different detunings of the diagonal, is provided in Extended Data Figure XD1. The panels on the left show the dynamics for zero interaction. In this case, Doublons cannot form and no joint dynamics through the bulk are observed. Increasing the detuning beyond the first resonance, whose associated dynamics are depicted in Fig. 4, results in unstable Doublons that decay during evolution by radiation into the bulk of the lattice. In turn, for very high interaction strength, even the off-resonant Doublon dynamics converge to the resonant ones.

Experimental data obtained by probing the four characteristics bands at the first resonance (see Fig. 3c) is shown in Extended Data Figure XD2. We examine the dispersion-free linear diffraction bands at the outer edge and the inner edge along the diagonal, the flat band of the bulk with compact localized states, and the Doublon flat-band formed by the lattice's main diagonal.

In our work, we explore the physics of interaction-induced two-particle topological states. We implement non-local interactions induced by a non-adiabatic periodic driving using a dimensional mapping procedure in an artificial photonic solid. With this approach, we are able to show the formation of Doublon quasi-particles at certain resonances in the interaction strength and demonstrate their topologically protected motion through the bulk of the system. Our results provide experimental evidence on the exceptional properties of Doublon particles in terms of their dynamics, topology, and resonant behavior, which are responsible for phenomena that are drastically distinct from the familiar single-particle realm. As such, our results have far-reaching consequences in a wide range of few-particle systems, as they offer an important step towards the experimental exploration of such phenomena.

## References

1. Kane, C. L. & Mele, E. J. Quantum Spin Hall Effect in Graphene. *Phys. Rev. Lett.* 95, 226801 (2005).
2. Bernevig, B. A. & Zhang, S.-C. Quantum Spin Hall Effect. *Phys. Rev. Lett.* 96, 106802 (2006).
3. König, M. et al. Quantum Spin Hall Insulator State in HgTe Quantum Wells. *Science* 318, 766–770 (2007).
4. Hasan, M. Z. & Kane, C. L. Colloquium : Topological insulators. *Rev. Mod. Phys.* 82, 3045–3067 (2010).
5. Ozawa, T. et al. Topological photonics. *Rev. Mod. Phys.* 91, 015006 (2019).
6. Haldane, F. D. M. Model for a Quantum Hall Effect without Landau Levels: Condensed-Matter Realization of the ‘Parity Anomaly’. *Phys. Rev. Lett.* 61, 2015–2018 (1988).
7. Jotzu, G. et al. Experimental realization of the topological Haldane model with ultracold fermions. *Nature* 515, 237–240 (2014).
8. Imhof, S. et al. Topoelectrical-circuit realization of topological corner modes. *Nat. Phys.* 14, 925–929 (2018).
9. Hadad, Y., Soric, J. C., Khanikaev, A. B. & Alù, A. Self-induced topological protection in nonlinear circuit arrays. *Nat. Electron.* 1, 178–182 (2018).
10. Süsstrunk, R. & Huber, S. D. Observation of phononic helical edge states in a mechanical topological insulator. *Science* 349, 47–50 (2015).
11. He, C. et al. Acoustic topological insulator and robust one-way sound transport. *Nat. Phys.* 12, 1124–1129 (2016).
12. Rechtsman, M. C. et al. Photonic Floquet topological insulators. *Nature* 496, 196–200 (2013).
13. Hafezi, M., Mittal, S., Fan, J., Migdall, A. & Taylor, J. M. Imaging topological edge states in silicon photonics. *Nat. Photonics* 7, 1001–1005 (2013).
14. Maczewsky, L. J., Zeuner, J. M., Nolte, S. & Szameit, A. Observation of photonic anomalous Floquet topological insulators. *Nat. Commun.* 8, 13756 (2017).
15. Mukherjee, S. et al. Experimental observation of anomalous topological edge modes in a slowly driven photonic lattice. *Nat. Commun.* 8, 13918 (2017).
16. Wintersperger, K. et al. Realization of an anomalous Floquet topological system with ultracold atoms. *Nat. Phys.* 16, 1058–1063 (2020).
17. Fritzsche, A. et al. Parity–time-symmetric photonic topological insulator. *Nat. Mater.* 1–6 (2024) doi:10.1038/s41563-023-01773-0.
18. Poli, C., Bellec, M., Kuhl, U., Mortessagne, F. & Schomerus, H. Selective enhancement of topologically induced interface states in a dielectric resonator chain. *Nat. Commun.* 6, 6710 (2015).
19. Blanco-Redondo, A., Bell, B., Oren, D., Eggleton, B. J. & Segev, M. Topological protection of biphoton states. *Science* 362, 568–571 (2018).
20. Mittal, S., Goldschmidt, E. A. & Hafezi, M. A topological source of quantum light. *Nature* 561, 502–506 (2018).
21. Kraus, Y. E., Lahini, Y., Ringel, Z., Verbin, M. & Zilberberg, O. Topological States and Adiabatic Pumping

- in Quasicrystals. *Phys. Rev. Lett.* 109, 106402 (2012).
22. Zilberberg, O. et al. Photonic topological boundary pumping as a probe of 4D quantum Hall physics. *Nature* 553, 59–62 (2018).
  23. Lohse, M., Schweizer, C., Price, H. M., Zilberberg, O. & Bloch, I. Exploring 4D quantum Hall physics with a 2D topological charge pump. *Nature* 553, 55–58 (2018).
  24. Mukherjee, S. & Rechtsman, M. C. Observation of Floquet solitons in a topological bandgap. *Science* 368, 856–859 (2020).
  25. Maczewsky, L. J. et al. Nonlinearity-induced photonic topological insulator. *Science* 370, 701–704 (2020).
  26. Jürgensen, M., Mukherjee, S., Jörg, C. & Rechtsman, M. C. Quantized fractional Thouless pumping of solitons. *Nat. Phys.* 19, 420–426 (2023).
  27. Pitaevskii, Lev P. Pitaevskii, Lev P. ‘Vortex lines in an imperfect Bose gas.’ *Sov. Phys. JETP* 13.2 (1961): 451–454.
  28. Bloch, I. Ultracold quantum gases in optical lattices. *Nat. Phys.* 1, 23–30 (2005).
  29. Winkler, K. et al. Repulsively bound atom pairs in an optical lattice. *Nature* 441, 853–856 (2006).
  30. Schreiber, M. et al. Observation of many-body localization of interacting fermions in a quasirandom optical lattice. *Science* 349, 842–845 (2015).
  31. Walter, A.-S. et al. Quantization and its breakdown in a Hubbard–Thouless pump. *Nat. Phys.* 19, 1471–1475 (2023).
  32. Barbiero, L., Menotti, C., Recati, A. & Santos, L. Out-of-equilibrium states and quasi-many-body localization in polar lattice gases. *Phys. Rev. B* 92, 180406 (2015).
  33. Di Liberto, M., Recati, A., Carusotto, I. & Menotti, C. Two-body physics in the Su-Schrieffer-Heeger model. *Phys. Rev. A* 94, 062704 (2016).
  34. Gorlach, M. A. & Poddubny, A. N. Topological edge states of bound photon pairs. *Phys. Rev. A* 95, 053866 (2017).
  35. Stepanenko, A. A. & Gorlach, M. A. Interaction-induced topological states of photon pairs. *Phys. Rev. A* 102, 013510 (2020).
  36. Berti, A. & Carusotto, I. Topological two-particle dynamics in a periodically driven lattice model with on-site interactions. *Phys. Rev. A* 105, 023329 (2022).
  37. Corrielli, G., Crespi, A., Della Valle, G., Longhi, S. & Osellame, R. Fractional Bloch oscillations in photonic lattices. *Nat. Commun.* 4, 1555 (2013).
  38. Mukherjee, S. et al. Observation of pair tunneling and coherent destruction of tunneling in arrays of optical waveguides. *Phys. Rev. A* 94, 053853 (2016).
  39. Tai, M. E. et al. Microscopy of the interacting Harper–Hofstadter model in the two-body limit. *Nature* 546, 519–523 (2017).
  40. Olekhno, N. A. et al. Topological edge states of interacting photon pairs emulated in a topoelectrical circuit. *Nat. Commun.* 11, 1436 (2020).
  41. Léonard, J. et al. Realization of a fractional quantum Hall state with ultracold atoms. *Nature* 619, 495–499

(2023).

42. Valiente, M. Lattice two-body problem with arbitrary finite-range interactions. *Phys. Rev. A* 81, 042102 (2010).
43. Bello, M., Creffield, C. E. & Platero, G. Long-range doublon transfer in a dimer chain induced by topology and ac fields. *Sci. Rep.* 6, 22562 (2016).
44. Su, W. P., Schrieffer, J. R. & Heeger, A. J. Solitons in Polyacetylene. *Phys. Rev. Lett.* 42, 1698–1701 (1979).
45. Malkova, N., Hromada, I., Wang, X., Bryant, G. & Chen, Z. Observation of optical Shockley-like surface states in photonic superlattices. *Opt. Lett.* 34, 1633–1635 (2009).
46. Longhi, S. Photonic Bloch oscillations of correlated particles. *Opt. Lett.* 36, 3248–3250 (2011).
47. Rudner, M. S., Lindner, N. H., Berg, E. & Levin, M. Anomalous Edge States and the Bulk-Edge Correspondence for Periodically Driven Two-Dimensional Systems. *Phys. Rev. X* 3, 031005 (2013).
48. Maczewsky, L. J. et al. Fermionic time-reversal symmetry in a photonic topological insulator. *Nat. Mater.* 19, 855–860 (2020).
49. Drücke, H., Meschede, M. & Bauer, D. Steering edge currents through a Floquet topological insulator. *Phys. Rev. Res.* 5, 023056 (2023).
50. Szameit, A. & Nolte, S. Discrete optics in femtosecond-laser-written photonic structures. *J. Phys. B At. Mol. Opt. Phys.* 43, 163001 (2010).



## Figures

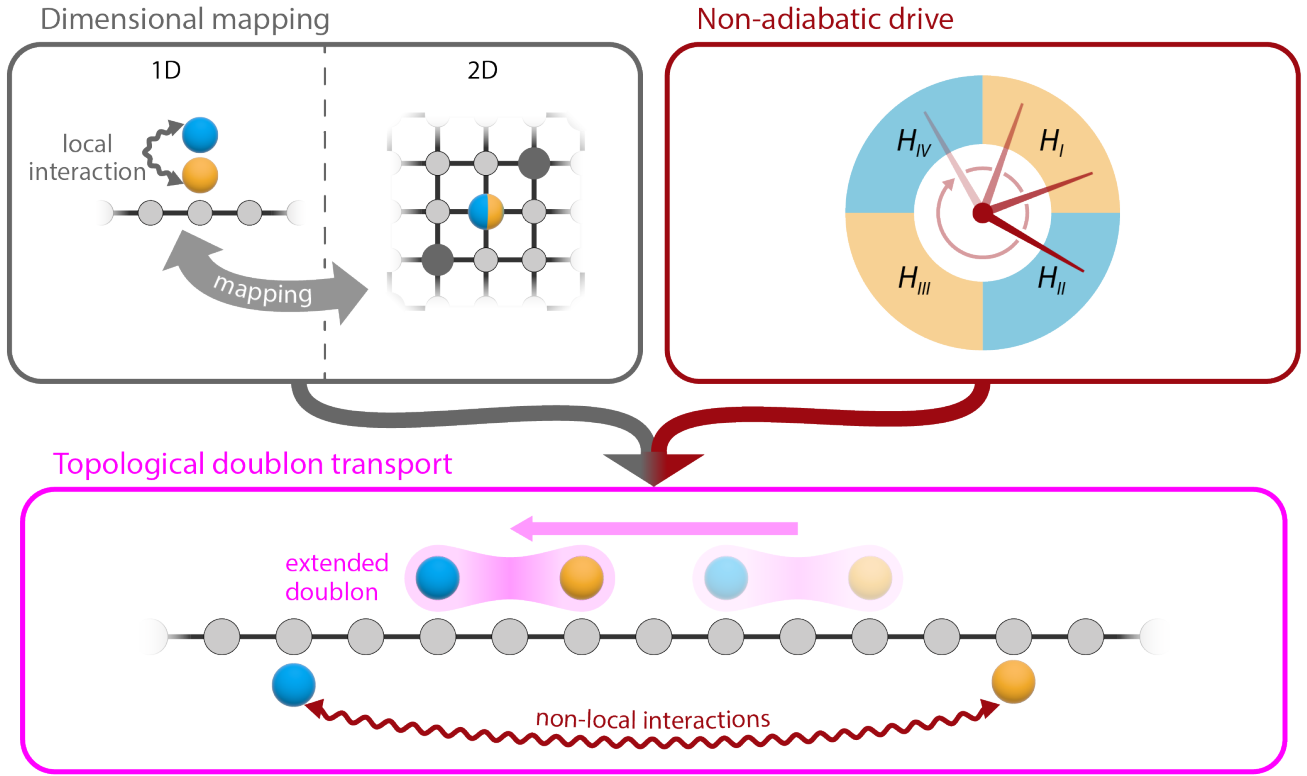


**Figure 1: Topological bulk transport of Doublons.** Dimensional mapping enables the observation of two-particle dynamics with local interactions in single-particle systems. The local interactions appear as onsite potentials along the diagonal in the 2D lattice. If the couplings of the 1D chain occur not simultaneously but in sequence according to a non-adiabatic periodic drive (see Supplementary Information), non-local interactions between the particles can also be induced, resulting in a non-trivial topology. The synergy between these two approaches allows the experimental observation of the topological transport of an extended two-particle bound state (so-called Doublon) through the bulk.

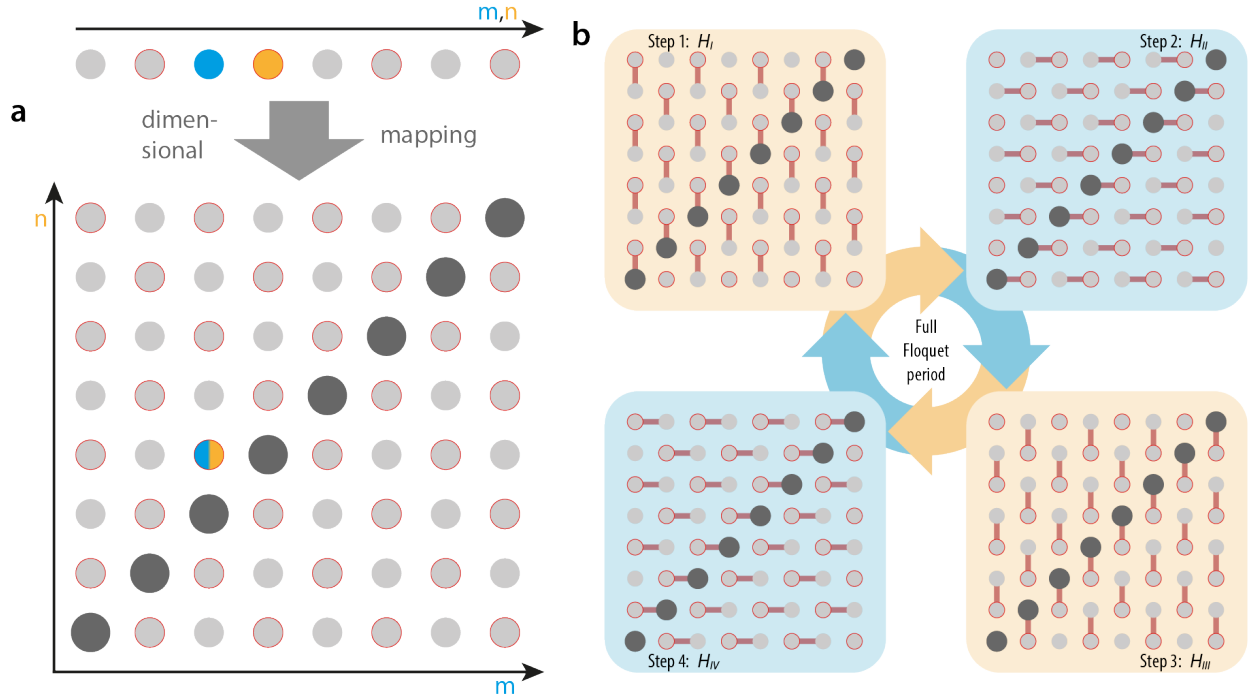


**Figure 2: Dimensional mapping.** (a) The dynamics of two interacting particle (orange and blue) with positions  $m$  and  $n$  on a 1D lattice can be mapped to a single particle on a corresponding square lattice. There the local interaction is governed by the onsite potential (highlighted by thick dark grey sites) of the diagonal sites, which are limited to the main diagonal in this case (Hubbard interactions). (b) The system is externally driven by applying a time periodic modulation to the couplings between both sublattices (indicated by red and grey outline) of the 2D lattice, according to the anomalous Floquet protocol. The protocol consists of four discrete couplings steps lasting for  $T/4$  of full period  $T$ , while the onsite potential of the sites stays constant over a full cycle. Each coupling step instantiates one of the virtual Hamiltonians  $\hat{H}_I, \dots, \hat{H}_{IV}$ , and the drive-induced delay between them ensures their non-local interactions dynamics remains intact.

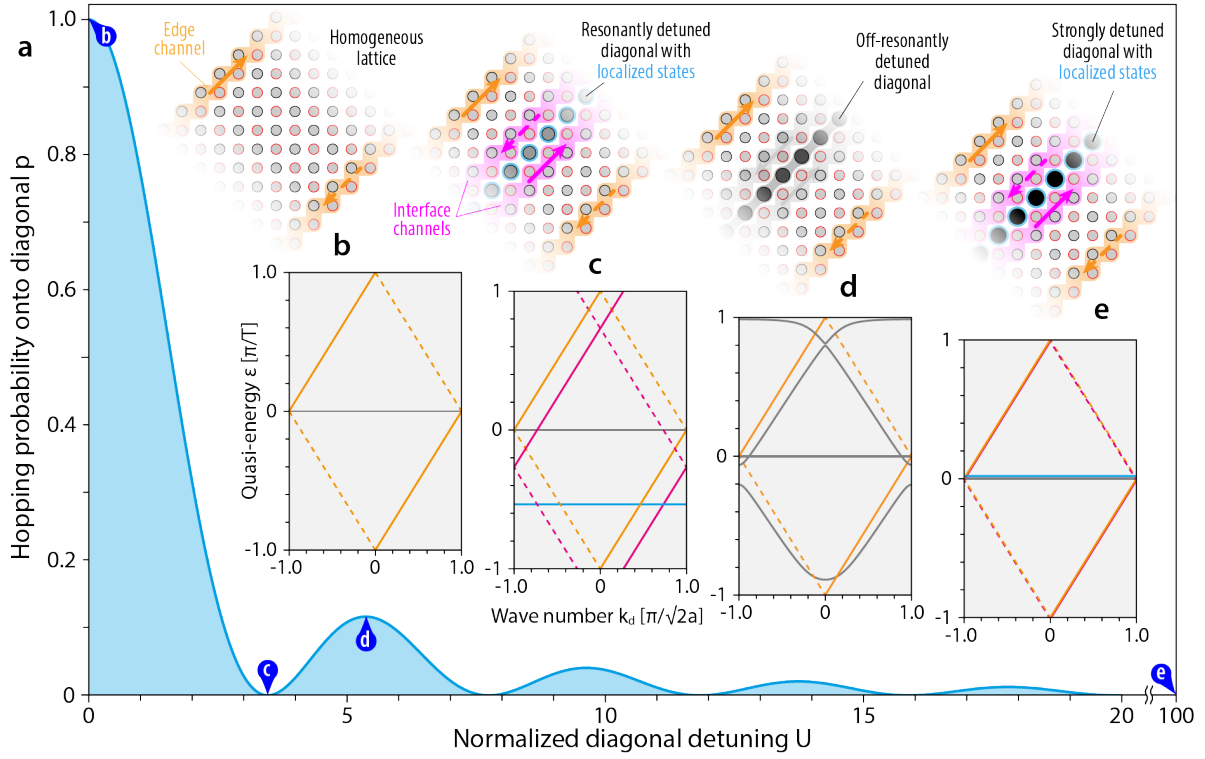


**Figure 3: Transfer probability and band structures.** (a) The hopping probability  $p(U)$  onto the lattice's diagonal possesses a decaying envelope but also vanishes for certain interaction strengths. (b) For zero detuning on the diagonal (analogous to vanishing interaction strength) an anomalous edge state (orange) bifurcates from the degenerate flat-bands at zero energy. (c) At the first zero of  $p(U)$  the lattices left and right of the diagonal decouple, resulting in additional interface channels with corresponding edge bands (pink). The states on the diagonal sites remain localized in the detuned flat-band (blue). (d) For non-zero detuning off the resonances, a superposition of three interface bands with avoided crossings forms. (e) When increasing the detuning towards infinity the (pink) interface bands and the conventional edge bands (orange) overlap in energy.

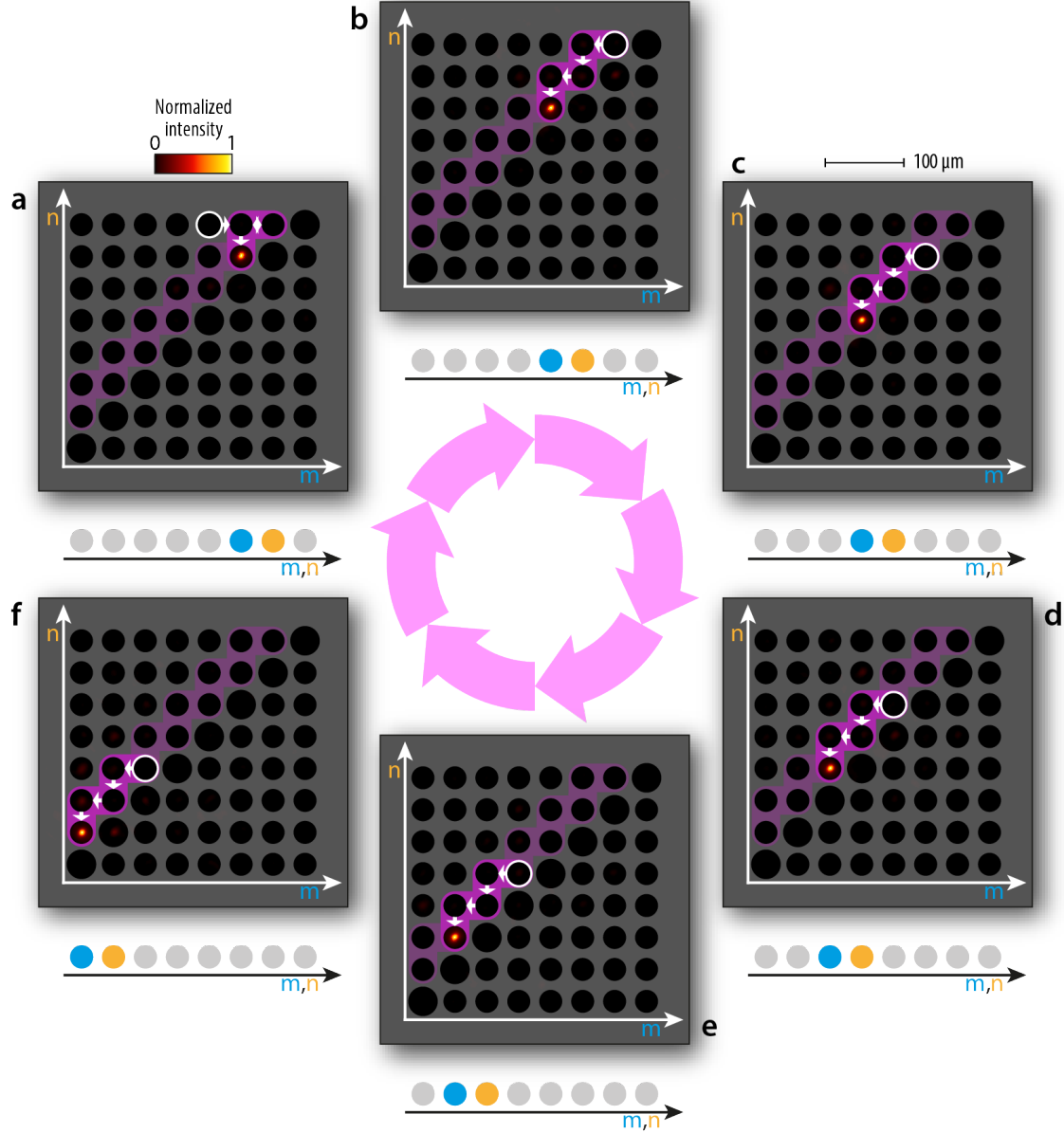


**Figure 4: Tracing the Doublon state at the first resonance.** The resonant system was successively probed experimentally by single-site excitations (white circles) along the off-diagonal of the square lattice. By setting the excitation to the output of the previous measurement panel, the movement of the edge state can be traced. **(a-f)** After two full Floquet periods the injected wave packet had propagated over four sites (i.e. two unit cells) adjacent to the lattices diagonal. When this process is mapped back onto the 1D lattice, a movement of the Doublon through the bulk to descending coordinates can be observed. The bound state remains constantly extended over two sites for all propagation distances. If periodic boundary conditions are assumed in the 1D grid, panel **f** would follow another instance of panel **a**.

## Methods

**Experimental configuration.** The photonic structures were fabricated using the femtosecond laser direct-writing method<sup>50</sup>. Ultrashort laser pulses emitted from a frequency-doubled fiber amplifier system (Coherent Monaco, wavelength 517 nm, repetition rate 333 kHz, pulse duration 270 fs) is focused into the volume of a fused silica sample (Corning 7980, dimensions 1 mm × 20 mm × 150 mm, bulk refractive index  $n_0 = 1.457$  at 633 nm), utilizing a 50x microscope (0.60 NA) objective. In the focal region, a permanent refractive index change is induced and, by moving the sample along arbitrary three-dimensional trajectories under the beam via a precision translation system (Aerotech ALS130), waveguides are formed. The resulting single-mode waveguides have a typical refractive index contrast of up to  $\Delta n_0 = 2 \cdot 10^{-3}$ .

The local particle interactions resembled by detuned waveguides on the diagonal of the 2D square lattice are created by inscribing these waveguides with different speeds between 35 and 120mm/min, respectively, as structures fabricated with lower speeds represent higher local interaction potentials. The non-local interactions, induced by non-adiabatic driving of the virtual Hamiltonians, is implemented via the anomalous driving scheme<sup>14,47</sup>, with two full Floquet periods  $T$ , by selectivity switching the nearest-neighbour hoppings using directional couplers. To achieve a non-trivial winding of  $W = 1$ , a hopping of  $J = \frac{2\pi}{T}$  is chosen, corresponding to a complete light transfer in each coupler. In the experimental realisation, this results in a  $J = 0.1189 \text{ mm}^{-1}$  for couplers of the length  $L = 13.211 \text{ mm}$ . In practice, the realized coupling ratios deviate slightly from the desired 100:0% ratio, with up to 4% of the light remaining in the excited waveguide, which has been accounted for in the theory curves depicted in Fig XD1c. The normalised detunings  $U$  used are the ratio of the absolute detuning  $\delta$  (determined from a detuning scan) to the coupling  $J$ . The propagation dynamics of the Doublon were probed with coherent light from a Helium-Neon laser (Melles Griot - 25mW), and measured after two Floquet periods using a CCD camera (Basler A120f).

**Numerical simulations.** The band structures (Fig. 2) are calculated numerically by solving the discrete Schrödinger equation as an eigenvalue problem. A finite grid strip (as shown in Fig. 2) with periodic boundary conditions in the direction of the wave vector was used for this purpose.

The theoretical target occupations from Fig. XD1 are obtained from computations of the respective field dynamics of the corresponding discrete Schrödinger equation.

## Data availability

The experimental and numerical data that support the findings of this study are available in an open-access data repository [reference follows].

## Author contributions

J.B. designed and fabricated the samples and performed the experiments. M.M., H.D., D.B. provided the theoretical foundations. J.B., F.P. performed the numerical simulations. S.W., J.F., M.H. provided analysis tools. A.S. supervised the project. All authors discussed the results and co-wrote the manuscript.

## **Acknowledgements**

We thank C. Otto for preparing the high-quality fused silica samples used for the inscription of all photonic structures employed in this work. A.S. acknowledges funding from the Deutsche Forschungsgemeinschaft (grants SZ 276/9-2, SZ 276/19-1, SZ 276/20-1, SZ 276/21-1, SZ 276/27-1, and GRK 2676/1-2023 ‘Imaging of Quantum Systems’, project no. 437567992). A.S. also acknowledges funding from the Krupp von Bohlen and Halbach Foundation as well as from the FET Open Grant EPIQUS (grant no. 899368) within the framework of the European H2020 programme for Excellent Science. A.S., M.H. and D.B. acknowledge funding from the Deutsche Forschungsgemeinschaft via SFB 1477 ‘Light–Matter Interactions at Interfaces’ (project no. 441234705).

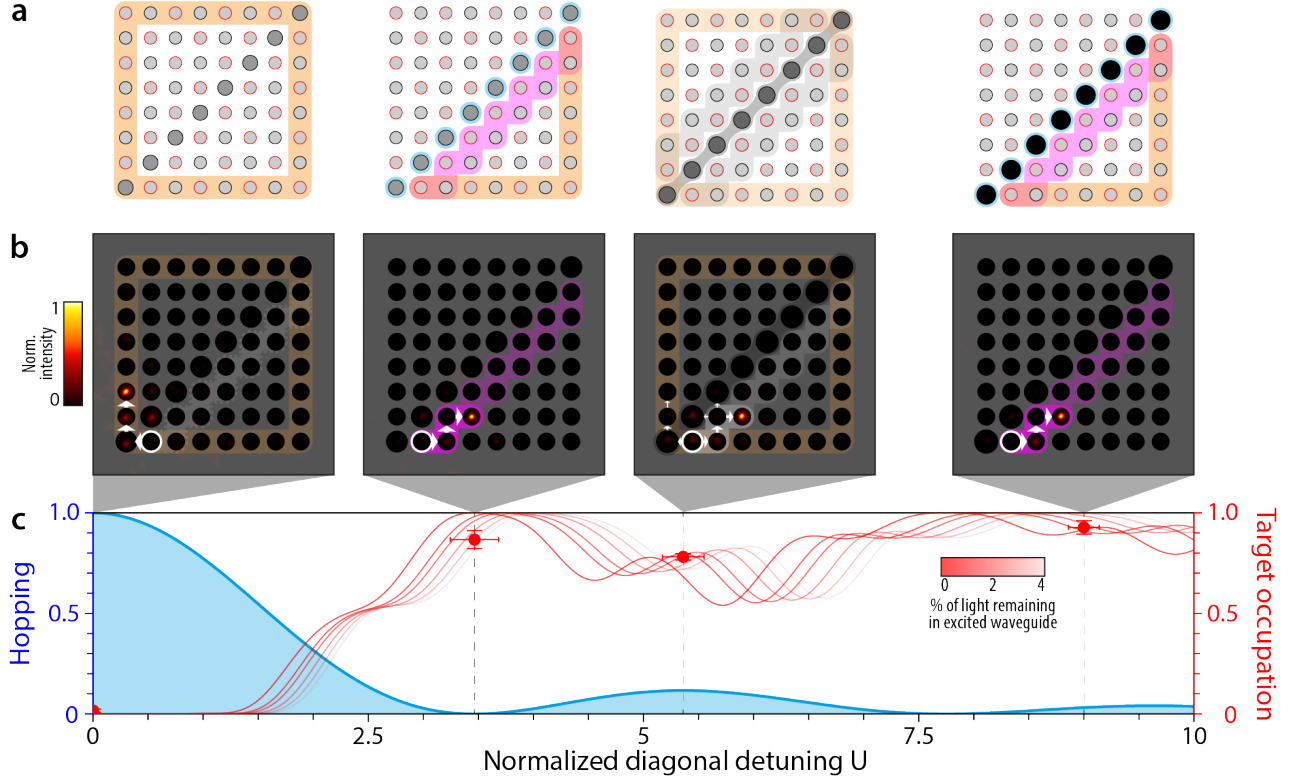
## **Competing interests**

The authors declare no competing financial interests.

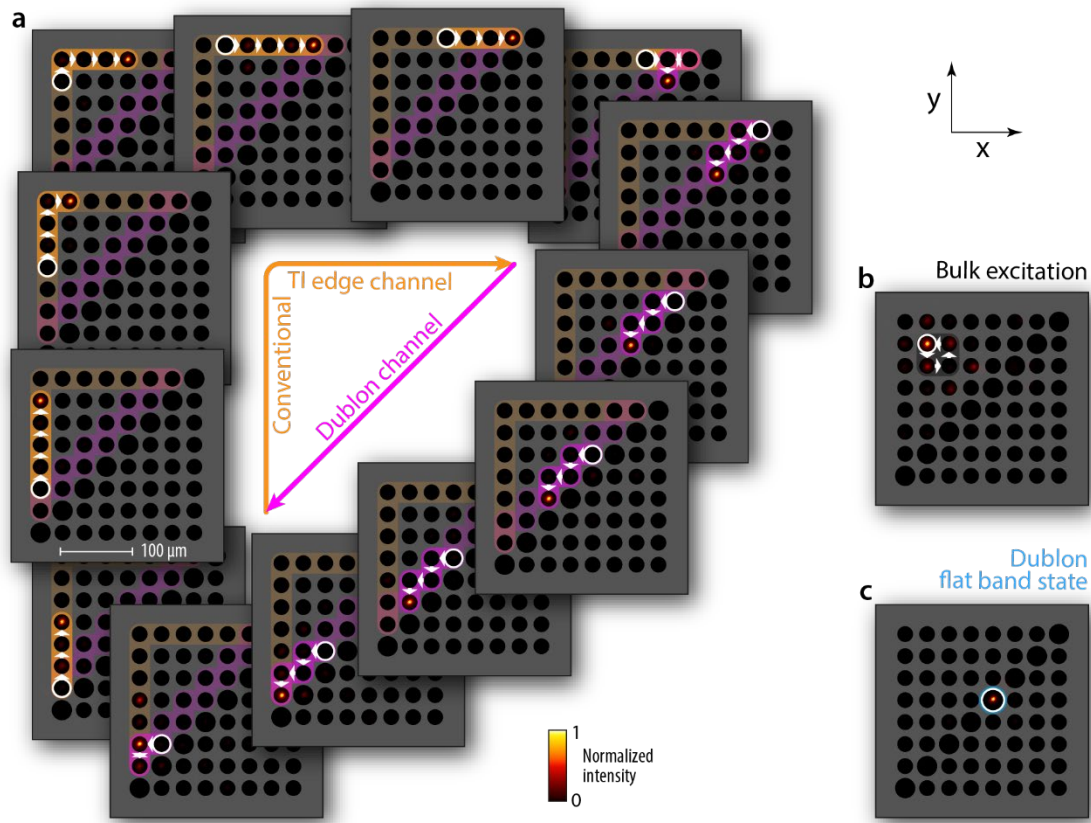
## **Materials & correspondence**

Correspondence and requests for additional materials should be addressed to A.S.

## Extended Data Figures



**Extended Data Figure XD1: Comparison of the dynamics for different interaction strength.** (a): Schematic representation of the pathways through which light can travel from the excitation. The compact localized states are indicated in blue, conventional topologically protected states in orange, and the Doublon edge state in pink. Meanwhile, non-topological channels are distinguished in grey. (b) Snapshot of the experimentally measured light propagation after two Floquet periods for various particle interaction potentials, when the white circled waveguide was populated. The light path is emphasized by arrows, where the line thickness is an indication of the coupling probability. (c) Illustration of the hopping probability onto the main diagonal in blue and the measured and simulated target occupation (definition see Supplementary Information) as a function of the interaction potential. The ratios were calculated from the measured images above. The solid theoretical curves of the target ratio emphasize the fluctuation range of the manufacturing accuracy of the targeted 100:0% directional couplers<sup>14</sup>.



**Extended Data Figure XD2: Tracing the edge propagation at the first resonance.** The four characteristic bands at the first resonance are probed experimentally. **(a)** To selectively populate the conventional edge channel, light is injected into a single site (encircled in white) along the outer edge of the square lattice. After two full Floquet periods, the wave packet has propagated over four sites (i.e. two unit cells) in clockwise direction along the edge. Both topological channels show unidirectional transport in a protected fashion even around the corners. **(b)** As a proof of principle when probing the bulk flat-band the wave packet remains quasi-localized after following the micromotion indicated by the arrows during one full Floquet period. **(c)** The Doublon flat-band state residing on the lattices main diagonal remains localized for strong interaction potentials and only shows micromotions within a Floquet step for finite potentials.